

Melting and freezing of spherical bismuth nanoparticles confined in a homogeneous sodium borate glass

G. Kellermann^{1,*} and A. F. Craievich²¹Laboratório Nacional de Luz Síncrotron, C.P. 6192, CEP 13083-970, Campinas, São Paulo, Brazil²Instituto de Física, Universidade de São Paulo, C.P. 66318, CEP 05315-970, São Paulo, São Paulo, Brazil

(Received 3 May 2008; revised manuscript received 8 July 2008; published 11 August 2008)

The melting temperature and the crystallization temperature of Bi nanoclusters confined in a sodium borate glass were experimentally determined as functions of the cluster radius. The results indicate that, on cooling, liquid Bi nanodroplets exhibit a strong undercooling effect for a wide range of radii. The difference between the melting temperature and the freezing temperature decreases for decreasing radius and vanishes for Bi nanoparticles with a critical radius $R=1.9$ nm. The magnitude of the variation in density across the melting and freezing transitions for Bi nanoparticles with $R=2$ nm is 40% smaller than for bulk Bi. These experimental results support a basic core-shell model for the structure of Bi nanocrystals consisting of a central crystalline volume surrounded by a structurally disordered shell. The volume fraction of the crystalline core decreases for decreasing nanoparticle radius and vanishes for $R=1.9$ nm. Thus, on cooling, the liquid nanodroplets with $R < 1.9$ nm preserve, across the liquid-to-solid transformation, their homogeneous and disordered structure without crystalline core.

DOI: 10.1103/PhysRevB.78.054106

PACS number(s): 64.70.Nd, 61.05.cf, 65.80.+n

I. INTRODUCTION

Metallic nanoparticles have been the object of a growing interest due to their often interesting chemical and physical properties.¹ A clear understanding of the structure and thermal behavior of these nanocrystals is worth because, in many cases, their properties are strongly dependent of the structure and structural stability of these nanomaterials. In a previous investigation² we have studied the crystal-to-liquid transition of spherical Bi nanoclusters embedded in a sodium borate glass as a function of the nanocrystal radius, by simultaneous small angle x-ray scattering (SAXS) and wide angle x-ray scattering (WAXS) experiments. In the present work, we have studied, by using the same experimental techniques, the whole cycle of heating and cooling of a similar Bi-glass nanocomposite, allowing us to determine both the liquid-to-crystal transition temperature T_c and the crystal-to-liquid transition temperature T_m and thus precisely characterize undercooling effects as a function of the nanocrystal radius. The procedure applied here,² in which a single sample is analyzed, yields experimental results with a good accuracy, even in the determination of small differences between $T_m(R)$ and $T_c(R)$, that have been here actually observed for very small nanoparticles.

The melting and the crystallization temperatures of spherical Bi nanoparticles were determined as functions of their radius by analyzing experimental data obtained from simultaneous measurements of SAXS and WAXS intensities. The measurements were performed *in situ*, on a single sample containing spherical Bi nanoclusters with a rather wide radius distribution, over the temperature range between 300 and 550 K.

II. EXPERIMENT

The glass sample containing Bi nanoparticles was prepared by using the melt-quenching technique followed by an

isothermal treatment at a temperature favoring a controlled nanoparticle growth.³ The raw material was a mixture of powdered Na_2CO_3 , B_2O_3 , Bi_2O_3 , and SnO . SnO was used as a reducing agent for Bi_2O_3 . The mixture of powders was melted in an electrical furnace under vacuum (10^{-1} mbar) at 1300 K during 1 h. The nominal composition of the melt after evaporation of volatiles, in the mol%, was $27\text{Na}_2\text{O}-69\text{B}_2\text{O}_3-\text{Bi}_2\text{O}_3-3\text{SnO}$. The melt was then fast quenched down to room temperature using the splat-cooling technique. As a result we have obtained a thin glass plate (150 μm thick) transparent to visible light in which Bi atoms were homogeneously dispersed.

An x-ray fluorescence analysis of a glass sample with the same composition as the glass matrix of the sample studied here, but prepared under air atmosphere, yielded essentially the same nominal composition.⁴ Nevertheless, in the present study, in which the raw material was melted under vacuum, some changes in composition may occur due to probable losses by evaporation. We have not chemically analyzed the Bi content of the studied Bi-glass nanocomposite. However, we previously determined the volume fraction of Bi nanoclusters from the results of measurements of SAXS intensity in absolute units.³ This volume fraction was determined to be $\sim 10^{-4}$, i.e., smaller than the fraction expected from the nominal Bi content. This indicates that the portion of melt poured into the splat-cooling device that yielded the studied glass thin plate is poorer in Bi than the average volume. This is a consequence from the expected effect of gravity that tends to concentrate the heavier Bi atoms near the bottom of the crucible. Anyway, the observed decrease in volume fraction of the Bi nanoclusters and the probable change in the matrix composition are not expected to significantly affect the conclusions of this investigation.

In order to promote the formation and growth of Bi liquid droplets the sample was annealed for 1 h at 823 K, well above the melting temperature of bulk Bi (544.5 K). Finally, in order to study the freezing (or crystallization) process, the

Bi nanocrystals-glass sample was cooled down to room temperature at a rate of 2.2 K/min and then heated at a rate of 2.3 K/min to also characterize the melting transition.

Our simultaneous *in situ* SAXS and WAXS study of the Bi nanocrystals confined in sodium borate glass was performed at the SAXS beamline of the Brazilian Synchrotron Light Laboratory (LNLS), Campinas, Brazil.⁵ SAXS and WAXS data were recorded using two one-dimensional gas x-ray position sensitive detectors. The SAXS intensity was measured as a function of the modulus of the scattering momentum transfer $q=4\pi \sin \theta/\lambda$; θ being half of the scattering angle and λ being the used wavelength of the x-ray beam (0.1608 nm).

III. RESULTS AND DISCUSSION

The SAXS power (in absolute units) of a diluted set of spherical nanoparticles with a spatially constant electron density ρ_p embedded in a homogeneous matrix with a constant electron density $\langle\rho\rangle$ is given by⁶

$$I_{\text{SAXS}}(q) = r_0^2(\rho_p - \langle\rho\rangle)^2 \left(\frac{4\pi}{3}\right)^2 \int_0^\infty N(R)[F(qR)]^2 R^6 dR, \quad (1)$$

where q is the modulus of the scattering vector, $r_0 = 0.281793 \times 10^{-14}$ m the classical electron radius, $N(R)dR$ the number of nanocrystals per unit volume with radius between R and $R+dR$, and $F(qR)$ is defined by⁶

$$F(qR) = 3 \frac{\sin(qR) - qR \cos(qR)}{(qR)^3}. \quad (2)$$

The radius distribution $N(R)$ is determined by measuring the scattering power and numerically solving Eq. (1).

We are also interested in determining the mass density of the nanoparticles as a function of the temperature T . The integral in the reciprocal space of the isotropic SAXS intensity at different temperatures is given by:⁶

$$Q_{\text{SAXS}}(T) = 4\pi \int_{q=0}^\infty I_{\text{SAXS}}(q, T) q^2 dq = 8\pi^3 r_0^2 [\rho_p(T) - \langle\rho\rangle]^2 \varphi(T) [1 - \varphi(T)]. \quad (3)$$

In our case the volume fraction occupied by the particles phase φ is very small (0.01%) and thus $\varphi(1-\varphi) \approx \varphi$. From the three-dimensional (3D) integrals $Q_{\text{SAXS}}(T)$ of the experimental SAXS intensity determined at different temperatures and by applying Eq. (3), we have derived the temperature dependence of the electron density of Bi nanoparticles ρ_p . The mass density of Bi nanoparticles is simply given by $\rho_m(T) = \rho_p(T)A/(N_A Z)$. A and Z being the Bi atomic weight and atomic number, respectively, and N_A the Avogadro number.

The analysis of the integrals of the main Bragg peak of WAXS spectra of crystalline Bi, determined at different temperatures, allowed us to calculate the variation of the volume fraction of crystalline nanoparticles V_c . The details of this procedure were described elsewhere.²

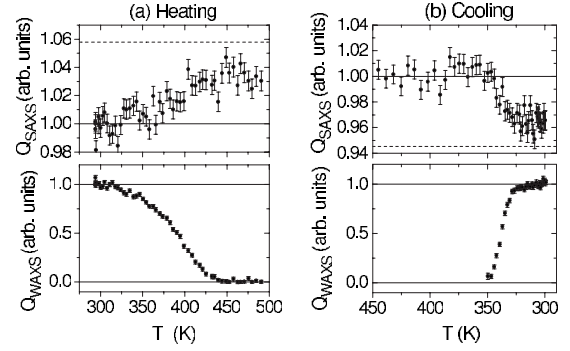


FIG. 1. Experimental SAXS and WAXS results during (a) heating and (b) cooling processes. Above: Integral of SAXS intensity in the reciprocal space Q_{SAXS} . Below: Integral of the main (012) Bi WAXS Bragg peak Q_{WAXS} . Q_{SAXS} and Q_{WAXS} before the phase transition (left-side of the curves) are normalized to unity. The horizontal dashed lines represent the Q_{SAXS} values expected for bulk Bi (a) after melting and (b) after crystallization. The relative variation expected for Q_{SAXS} through the whole phase transition assuming the density of the Bi nanoparticles equals to that of bulk Bi is $\sim 6\%$.

Figure 1 displays the 3D integral of SAXS curves $Q_{\text{SAXS}}(T)$ and the integral of the main crystalline Bi (012) Bragg peak $Q_{\text{WAXS}}(T)$ as functions of the temperature for both heating [Fig. 1(a)] and cooling [Fig. 1(b)] processes. A continuous decrease in the integral of the main Bi (012) Bragg peak associated to the progressive melting of the nanocrystals is observed in Fig. 1(a) (below) over the same temperature range (325–425 K), for which a continuous increase in the $Q_{\text{SAXS}}(T)$ function can also be noticed in Fig. 1(a) (above). This implies that the melting of the whole set of nanocrystals takes place over a wide range of temperature (~ 100 K). This obviously occurs because Bi nanoparticles with different radius melt at different temperatures.²

Since the density of crystalline Bi at the melting temperature (9.649 g/cm³) is lower than the density of liquid Bi (10.050 g/cm³), the radius of the nanoparticles are expected to increase during solidification and decrease during the melting transition. The increase in the Q_{SAXS} value of the sample under heating [Fig. 1(a), above] is the expected consequence of the increase in the mass density of the nanoparticles, and thus of $\Delta\rho^2 = (\rho_p - \langle\rho\rangle)^2$, during the crystals melting transition. An opposite behavior—increasing trend of the integral of the Bi (012) Bragg peak [Fig. 1(b), below] and simultaneous decreasing trend of the integrated SAXS intensity [Fig. 1(b), above]—is observed during the cooling process. This last (freezing) transformation, however, occurs at lower temperatures and over a range about three times smaller (~ 30 K) than that observed for the whole melting transition (~ 100 K).

From the variation in the integral of SAXS intensity Q_{SAXS} through the whole melting transition that was experimentally determined [Fig. 1(a), above], the relative variation in mass density of the Bi nanoparticles $\Delta\rho_m/\rho_m$ was derived ($\Delta\rho_m/\rho_m = 0.019 \pm 0.003$). This variation is about 40% smaller than the expected variation for mass density of bulk Bi [$\Delta\rho_m/\rho_m(\text{bulk}) = 0.0311$]. Nearly the same (in this case negative) variation is observed for the crystallization transition [Fig. 1(b), above].

These experimental SAXS results support a previously proposed simple structural model⁷ for which the nanocrystals are heterogeneous, i.e., they are composed of two phases, namely, a crystalline core and an external disordered shell. We will name it as the core-shell model. Under this assumption, our experimental results can be nicely understood because only the crystalline core (and not the whole volume) would noticeably change its mass density through the melting and crystallization transitions.

The size distribution of the set of spherical Bi nanoparticles confined in the borate glass sample studied here $N(R)$ —derived from the experimental profile of the SAXS pattern by numerically solving Eq. (1)—is a single-mode function with radii ranging from about 1.1 nm up to 4.2 nm and an average radius $\langle R \rangle$ equal to 2.30 ± 0.01 nm. The relative radius dispersion $\sigma/\langle R \rangle = 0.21 \pm 0.01$ calculated from the radius distribution function $N(R)$ is equivalent to the value predicted by the theoretical model proposed by Lifshitz and Slyosov⁸ and Wagner⁹ that describe the growth of the nanoparticles along the coarsening stage.

A careful analysis of the SAXS intensity curves recorded at different temperatures, in 300–550 K range during heating and cooling processes, indicates the presence of slight changes in the scattering profiles. In fact, small changes are actually expected as a consequence of the variation in nanoparticle mass density and consequently in the droplet radii during melting and crystallization. Due to the small variation in the volume during the liquid-to-solid and solid-to-liquid phase transitions, this contraction only slightly affects the radius distribution of the particles determined from Eqs. (1) and (2).

The radius dependences of the melting and freezing temperatures of spherical Bi nanoparticles were derived from the temperature dependence of the volume fraction of crystalline Bi $V_c(T)$ and the radius dependence of the volume fraction of crystalline Bi $V_c(R)$. These functions were determined from experimental WAXS and SAXS data, respectively, as described elsewhere.²

Figure 2 displays the melting and freezing temperatures—derived from our SAXS and WAXS measurements—as functions of the inverse of Bi nanoparticle radius ($1/R$), together with previous results reported in the literature for the radius dependence on the melting temperature of Bi nanoparticles supported on carbon film^{10,11} and embedded in a sodium borate glass.¹² Our experimental results plotted as T_m versus $1/R$ exhibit a clearly linear behavior as theoretically predicted by Couchman and Jesser.¹³ We can qualitatively remark in Fig. 2 that most of the melting temperatures of Bi nanocrystals reported in the literature exhibit a depression that is stronger for progressively smaller nanocrystals. The magnitude of the slope of the straight line in the $T_m \times 1/R$ plot reported by Itoigawa *et al.*¹² is higher than the slopes determined in the present study and also in our previous investigation of the same material.² We have tentatively assigned this discrepancy to the probable effect in the Itoigawa *et al.* study of systematic errors induced by nanocrystal size dispersion. These systematic errors are absent in the present work in which the procedure described in Ref. 2 was applied. We can also remark that our data in the $T_m \times 1/R$ plot linearly extrapolated toward small $1/R$ values are in good

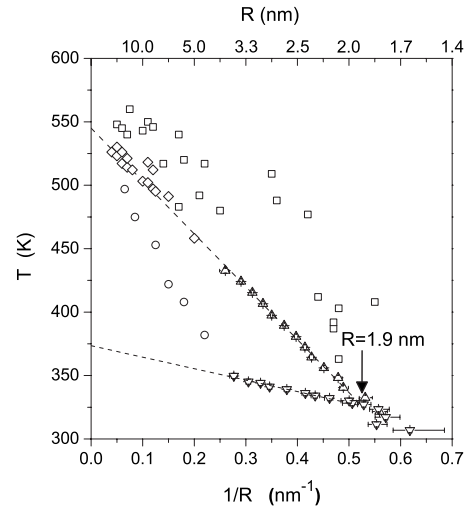


FIG. 2. Melting temperature (Δ) T_m and freezing temperature (∇) T_c of Bi nanoparticles embedded in a sodium borate glass as functions of their reciprocal radius $1/R$. The two straight lines were determined by weighted linear regression. Melting temperatures previously determined by other authors for Bi nanocrystals supported on carbon film—(\square) Peppiatt (Ref. 10) and (\diamond) Allen *et al.* (Ref. 11)—and embedded in the same glass—(\circ) Itoigawa *et al.* (Ref. 12)—are also plotted.

agreement with those obtained by Allen *et al.*¹¹ for the melting temperature of larger Bi nanocrystals. Data reported by Peppiatt,¹⁰ however, exhibit a rather large dispersion and do not indicate a well-defined radius dependence of the melting temperature.

Our results displayed in Fig. 2 clearly indicate that the melting temperature decreases for decreasing radius and is a linear function of $1/R$, i.e., $T_m = T_{mb} - a/R$, where T_{mb} is the melting temperature of bulk Bi crystals, in agreement with the results of our previous investigation.² This type of linear behavior displayed in Fig. 2 was theoretically proposed by Couchman and Jesser¹³ using a simple thermodynamic model. According to this theory, a is related to surface energy parameters. We have established for Bi nanocrystals with $R=2$ nm that the $(T_{mb} - T_m)$ difference is as much as about 200 K.

The crystallization or freezing temperature of bulk Bi T_{cb} is lower than T_{mb} ($\Delta = T_{mb} - T_{cb} = 151$ K). Our experimental results (Fig. 2) indicate that the freezing temperature of Bi droplets T_c decreases even more for decreasing nanodroplet radius. The temperature $T_c(1/R)$ decreases linearly for increasing $(1/R)$ at a lower rate than $T_m(1/R)$, in such a way that the difference $(T_m - T_c)$ progressively decreases for decreasing radius. The linear dependence of T_c on $(1/R)$ displayed in Fig. 2 can also be explained by using a previously proposed thermodynamic two-phase core-shell model.¹⁴

Within the accuracy of our experimental results (Fig. 2) we can conclude that Bi nanoparticles with radius equal to or smaller than about 1.9 nm melt and freeze at about the same temperature. The vanishing of the difference between the melting and freezing temperatures was previously observed also for very small Pb particles ($R \leq 2.5$ nm) confined in an alumina matrix¹⁵ and for CuCl nanoparticles ($R \leq 1.4$ nm) embedded in glass.¹⁶

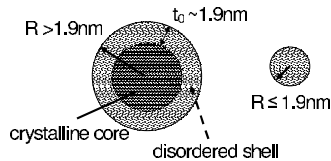


FIG. 3. Schematic model for the structure of Bi nanocrystals. Left: Nanocrystal with $R > 1.9$ nm composed of a crystalline core surrounded by a disordered shell. Right: Nanocrystal with $R \leq 1.9$ nm with only a homogeneous and disordered volume.

The coincidence of the melting and freezing temperatures for very small nanoparticles (below a well-defined or critical radius) can be understood in terms of the thermodynamic behavior of the surfaces established in previous studies.^{17–22} According to Kofman *et al.*,²³ for very small nanoparticles composed of a crystalline core and an external disordered shell—for which the thickness of the surface layer t_0 approaches the value of the nanoparticle radius R (see Fig. 3)—the effect of the external disordered shell is expected to be predominant. On the other hand, for nanoparticles with increasing radius, for which also a bulklike core and a disordered surface shell coexist, the bulk characteristics become progressively more dominant and thus the difference between the freezing and the melting temperatures is expected to progressively increase.

As the nanoparticle radii approach macroscopic values ($1/R \rightarrow 0$) the asymptotic melting and freezing temperatures are expected to become equal to those observed for bulk material. Our results plotted in Fig. 2 indicate that the melting temperature that we have determined by extrapolating $T_m(1/R)$ down to $1/R=0$, (545 ± 3)K, agrees well with the known value for bulk Bi ($T_{mb}=544.5$ K).

On the other hand, the freezing temperature of bulk Bi T_{cb} , that we have determined by linearly extrapolating $T_c(1/R)$ to $1/R \rightarrow 0$, according to a previous theoretical model,¹⁴ yields $T_{cb'}=374$ K; this value being 19 K lower than the freezing temperature of macroscopic volumes of liquid Bi [$T_{cb}=393$ K (Ref. 14)]. The reason for this discrepancy can be assigned to (i) an intrinsic limitation of the simple core-shell model used here to describe the crystal melting of very small nanoparticles, and/or to (ii) the inherent low accuracy of the crystallization temperature experimentally determined for undercooled bulk liquids; the eventual presence of impurities promoting heterogeneous nucleation and thus decreasing the undercooling effect.

The radius of the smallest nanocrystals retaining their essential crystalline structure was estimated in a previous work to be approximately $R_c=3h$, where h is the value of the spacing between atomic layers.²⁴ In the case of Bi $h=0.4072$ nm,²⁵ thus yielding $R_c \sim 1.2$ nm. Taking into account the rather simplified nature of the proposed model, this value is in good agreement with the value $R=1.9$ nm derived from our experimental results.

IV. CONCLUSION

The main conclusions regarding the radius dependence of the structural features and the melting and freezing temperatures of spherical Bi nanoparticles confined in a sodium borate glass are as follows: (i) The magnitudes of the relative changes in the average mass density of Bi nanoparticles during nanocrystal-to-liquid and liquid-to-nanocrystal transitions were determined to be 40% lower than for bulk Bi. This result supports the simple structural core-shell model for spherical nanocrystals, i.e., a crystalline central core surrounded by a rather disordered shell with a mass density close to the density of the liquid phase. (ii) The melting and the crystallization temperatures of Bi clusters exhibit a linear dependence on the inverse of nanoparticle radius ($1/R$), both straight lines meeting at a critical radius $R_c=1.9$ nm, at which the difference (T_m-T_c) vanishes. This finding is also consistent with the simple core-shell model described above. (iii) The features of the simple core-shell model suggest that, for very small Bi nanoparticles with $R < 1.9$ nm, the volume of the crystalline core vanishes so as the whole nanoparticle exhibits a disordered (noncrystalline) structure. Thus, for Bi nanoparticles with $R < 1.9$ nm, the liquid-to-solid and solid-to-liquid transitions become continuous transformations between two homogeneous and disordered structures without crystalline core. (iv) The radius of Bi nanodroplets below which no crystallization occurs ($R_c=1.9$ nm) can be considered as the critical radius for homogeneous crystal nucleation. This connection was previously argued by Jackson and McKenna²⁶ to explain the absence of crystallization for very small molecular clusters confined in a glass containing nanopores with subcritical sizes.

ACKNOWLEDGMENTS

This work was supported by LNLs and by Brazilian funding agencies PRONEX/CNPq and FAPESP.

*Author to whom correspondence should be addressed. Present address: Laboratório Nacional de Luz Síncrotron, C.P. 6192, CEP 130 83-970 Campinas, Sao Paulo, Brazil: keller@lnls.br

¹F. Gonella and P. Mazzoldi, *Handbook of Nanostructured Materials and Nanotechnology* (Academic, New York, 2000).

²G. Kellermann and A. F. Craievich, *Phys. Rev. B* **65**, 134204 (2002).

³G. Kellermann and A. F. Craievich, *Phys. Rev. B* **67**, 085405 (2003).

⁴H. Itoigawa, T. Kamiyama, and Y. Nakamura, *J. Non-Cryst. Solids* **220**, 210 (1997).

⁵G. Kellermann, F. Vicentin, E. Tamura, M. Rocha, H. Tolentino, A. Barbosa, A. F. Craievich, and I. L. Torriani, *J. Appl. Crystallogr.* **30**, 880 (1997).

⁶O. Glatter and O. Kratky, *Small Angle X-Ray Scattering* (Academic, London, 1982).

⁷C. M. R. Wronski, *Br. J. Appl. Phys.* **18**, 1731 (1967).

⁸I. M. Lifshitz and V. V. Slyozov, *J. Phys. Chem. Solids* **19**, 35

- (1961).
- ⁹C. Wagner, *Z. Elektrochem.* **4**, 581 (1961).
- ¹⁰S. J. Peppiatt, *Proc. R. Soc. London, Ser. A* **345**, 401 (1975).
- ¹¹G. L. Allen, R. A. Bayles, W. W. Gile, and W. A. Jesser, *Thin Solid Films* **144**, 297 (1986).
- ¹²H. Itoigawa, T. Kamiyama, and Y. Nakamura, *J. Non-Cryst. Solids* **210**, 95 (1997).
- ¹³P. R. Couchman and W. A. Jesser, *Nature (London)* **269**, 481 (1977).
- ¹⁴H. W. Sheng, K. Lu, and E. Ma, *Acta Mater.* **46**, 5195 (1998).
- ¹⁵P. Cheyssac, R. Kofman, and R. Garrigos, *Phys. Scr.* **38**, 164 (1988).
- ¹⁶P. M. Valov and V. I. Leĭman, *JETP Lett.* **66**, 510 (1997).
- ¹⁷G. L. Allen and W. A. Jesser, *J. Cryst. Growth* **70**, 546 (1984).
- ¹⁸Y. Lereah, G. Deutscher, P. Cheyssac, and R. Kofman, *Europhys. Lett.* **12**, 709 (1990).
- ¹⁹R. Garrigos, P. Cheyssac, and R. Kofman, *Z. Phys. D: At., Mol. Clusters* **12**, 497 (1989).
- ²⁰Z. B. Güvenç and J. Jellinek, *Z. Phys. D: At., Mol. Clusters* **26**, 304 (1993).
- ²¹Y. Qi, T. Çağın, W. L. Johnson, and W. A. Goddard III, *J. Chem. Phys.* **115**, 385 (2001).
- ²²F. Delogu, *Phys. Rev. B* **72**, 205418 (2005).
- ²³R. Kofman, P. Cheyssac, and R. Garrigos, *Phase Transitions* (Gordon and Breach, London, 1990), Vols. 24–26, pp. 330–336.
- ²⁴F. G. Shi, *J. Mater. Res.* **9**, 1307 (1994).
- ²⁵L. H. Liang, J. C. Li, and Q. Jiang, *Physica B (Amsterdam)* **334**, 49 (2003).
- ²⁶C. L. Jackson and G. B. McKenna, *Chem. Mater.* **8**, 2128 (1996).